Nonlocal Nuclear Spin Quieting in Quantum Dot Molecules: Optically Induced Extended Two-Electron Spin Coherence Time

Colin M. Chow, Aaron M. Ross, Danny Kim, Daniel Gammon, Allan S. Bracker, L. J. Sham, and Duncan G. Steel

Phys. Rev. Lett. **117**, 077403 — Published 12 August 2016

DOI: 10.1103/PhysRevLett.117.077403

Non-local nuclear spin quieting in quantum dot molecules: Optically-induced extended two-electron spin coherence time

Colin M. Chow[1,2,*], Aaron M. Ross[1,*], Danny Kim[3],
Daniel Gammon[3], Allan S. Bracker[3], L. J. Sham[4], Duncan G. Steel[1,2,*]
[1]H. M. Randall Laboratory of Physics, University of Michigan, Ann Arbor, Michigan
[2]Electrical Engineering and Computer Science, University of Michigan, Ann Arbor, Michigan
[3]Naval Research Laboratory, Washington D.C.
[4]Department of Physics, University of California San Diego, La Jolla, California
[*]These authors contributed equally to this work.

We demonstrate the extension of coherence between all four two-electron spin ground states of an InAs quantum dot molecule (QDM) via non-local suppression of nuclear spin fluctuations in two vertically stacked quantum dots (QDs), while optically addressing only the top QD transitions. Long coherence times are revealed through dark-state spectroscopy as resulting from nuclear spin locking mediated by the exchange interaction between the QDs. Lineshape analysis provides the first measurement of the quieting of the Overhauser field distribution correlating with reduced nuclear spin fluctuations.

The solid state community has made great strides in demonstrating basic quantum information operations using self-assembled quantum dot structures. Ground state initialization has been achieved in both electron[1, 2] and hole[3] spin systems, coherent spin rotations can be performed within picoseconds using detuned Raman pulses[4–6], spin states can be read out via absorption[6] or fluorescence[4, 7], and spin-photon entanglement[7–9] allows for the incorporation of these systems into quantum networks. The decoherence properties of electron and hole spin qubits have been investigated with data indicating that nuclear spin fluctuations via hyperfine coupling and residual charge fluctuations[10–13] are the primary sources of spin decoherence. Intense efforts have focused on how to protect the electron spin qubit from these noise sources, resorting to Hahn spin echo using ultrafast pulses[14] and nuclear spin fluctuation quieting[15, 16].

The fabrication of vertically-stacked self-assembled quantum dot molecules (QDMs)[17] has allowed the community to extend these studies to multi-dot systems. Progress has been made in the coherent control of two electrons trapped in a QDM consisting of two quantum dots separated by a small tunneling barrier[18, 19]. In such a two-electron system, a qubit is formed from the singlet S and the spin-projection zero triplet T_0 due to their relative insensitivity to charge and nuclear spin noise fluctuations. Ultrafast optical manipulation of the $S - T_0$ qubit has been demonstrated[20], later followed by coherent population trapping (CPT) experiments, revealing coherence times of at least 200 ns[21].

In this Letter, we report that dark-state spectroscopy reveals long coherence times for arbitrary superpositions of any of the four coupled-dot ground states $(S, T_0, T_\pm)$ of the two-electron strongly-coupled QDM system. The use of optical excitation of only one constituent dot of the QDM means that the quieting of the nuclear spin fluctuations which strengthens the spin coherence extends to the other dot. We interpret this non-local quieting as due to the strength of the coupled-dot spin states arising from the strong tunneling exchange between dots. Thus, in each quantum dot the mechanism of the nuclear spin bath driving the electron spin decoherence is dominated by that of an isolated QD[13, 15] in the presence of the Knight field on the dot regardless of whether the field is from the direct optical excitation of the electron spin in the dot or through the tunneling exchange. Nuclear spin diffusion from dot to dot is prevented by the nuclear spin energy mismatch through the tunnel barrier [13]. Analysis of the data provides the first measurement of the quieting of the Overhauser field distribution coinciding with the enhanced electron spin coherence time. We report a lower-bounded ground state coherence time of at least 1.3 microseconds. The implication for quantum information processing is the extension of the QDM platform beyond a single qubit (S-T_0) to a coupled two-qubit system or a qudit (d=4) system.

In the set of experiments described below, we study an InAs/GaAs QDM consisting of two InAs quantum dots separated by a small tunneling barrier embedded within a Schottky diode [18][22]. All absorption spectra are measured using Stark shift modulation spectroscopy at 6 K in a 1.5 T Voigt geometry magnetic field [22].

With an appropriate bias voltage, two electrons are confined in the QDM such that the wave function of each electron resides mostly in separate dots[18]. The tunneling of each electron through the inter-dot barrier leads to the Heisenberg exchange interaction which forms the molecular states. Hence, the two-electron states consist of the spin-singlet S and the triplet manifold, denoted by T_-, T_0, T_+, representing total spin down (m_j = -1), zero ($m_j = 0$) and up ($m_j = +1$), respectively. Using reso-

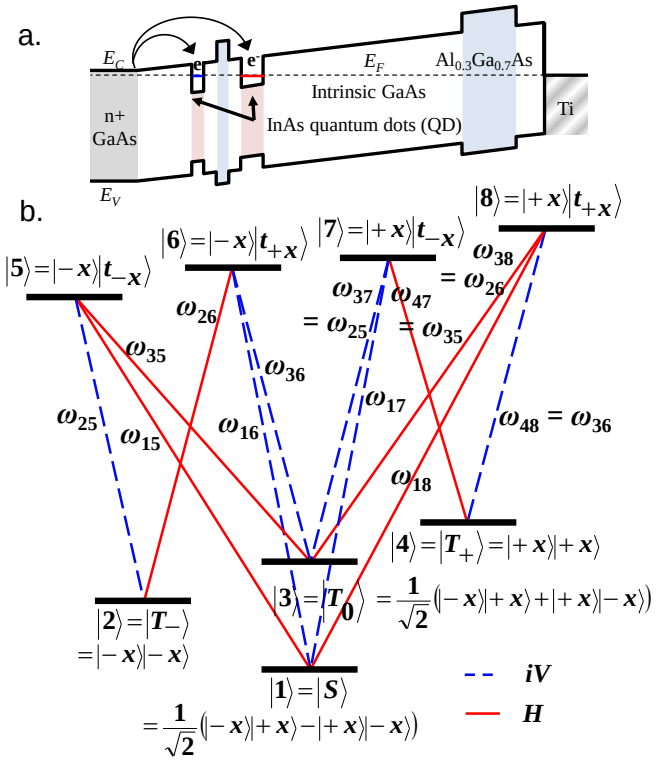

FIG. 1. a. Schematic of Schottky diode structure with quantum dot molecule. Vertical stacking order is from left to right. E_C,E_V,E_F are the conduction band energy, valence band energy and Fermi energy. b. Energy level diagram and optical transitions between singlet/triplet ground states and excited states in the presence of an in-plane (Voigt geometry) magnetic field. States consist of an electron in the lower QD, represented by $|\pm x\rangle$, and a trion in the top QD, represented by $|t_{\pm x}\rangle$. Spin projections are shown along +x-direction and +(−) denotes spin up (down). Blue/dashed (red/solid) lines represent vertical (horizontal) polarization.

nant excitation, an exciton is created in the top QD during optical excitation. The Coulomb interaction associated with this additional exciton prevents tunneling[18], thereby isolating the QDs. The optical excited states consist of a single electron in the lower QD and a trion, i.e., a heavy-hole and two spin-paired electrons, in the top QD, in which the spin state of the trion is given by the heavy-hole.

The S and T_0 states form the decoherence-free subspace which is immune to fluctuations of the nuclear Overhauser field from the underlying lattice. Ideally, in zero or an out-of-plane magnetic field (Faraday geometry), T_- and T_+ states are decoupled from the S-T_0 subspace. Nonetheless, weak coupling may arise due to an in-plane Overhauser field or heavy-hole-light-hole mixing[15], and could contribute to decoherence since T_- and T_+ states are susceptible to fluctuations of Overhauser field. Alternatively, as shown in Fig. 1, an in-plane magnetic field (Voigt geometry) splits the triplets and allows T_- and T_+ states to be coupled to the S-T_0 subspace via $\mathbf{\Lambda}$-systems. This offers the following advantages. First, ultrafast spin preparation of T_- and T_+ states can be achieved with optical pumping. Second, easy access to T_- and T_+ states enables nuclear spin locking via hyperfine coupling between the electron and nuclear spins; *We exploit this feature to extend the two-qubit coherence by over two orders of magnitude.*

The optically accessible system has four pairs of energetically degenerate transitions, $(\omega_{25},\omega_{37})$, $(\omega_{26},\omega_{38})$, $(\omega_{35},\omega_{47})$ and $(\omega_{36},\omega_{48})$. The experiments are performed in the regime in which the exchange splitting is independent of the bias voltage. Therefore, the contribution to the electron g-factors from the interdot AlGaAs barrier is negligible, leading to an experimentally indistinguishable difference between electron g-factors in the dots and therefore degenerate transition pairs. (Figure 1) [23, 24]. An out-of-equilibrium population of the T_+ state is achieved by the application of horizontally-polarized cw Pump 1 and 2, on resonance with transitions ω_{15} and $\omega_{26/38}$, respectively, as shown in Fig. 2a. By tuning the frequency of Pump 1 to ω_{15}, coherent population trapping (CPT)[25] is avoided and the system is prepared in T_+ state with near unity fidelity, confirmed by measuring an absorption signal only at ω_{48}. When the frequency difference between the probe and Pump 2 equals the Zeeman splitting of the triplets, CPT is expected, as demonstrated by a dark-state dip in the probe absorption spectrum. However, in both forward (increasing in frequency) and backward (decreasing in frequency) scans, the absorption spectra (Fig. 2b) exhibit distortion and hysteresis typical of dynamic nuclear spin polarization (DNSP). The spectra reveal the tuning of the optical resonance and, consequently, the two-photon resonance due to the shifting Overhauser field caused by the scanning of the probe. The optical resonance moves away when the scanning probe approaches, resulting in an abrupt reduction of the absorption signal. In the other case where the system is prepared in T_- state, the resonance appears to follow the scanning of the probe over a range of 10 μeV. [22]

Here we demonstrate suppression of the effects of DNSP due to the probe, thereby extending the decoherence time of the two-electron ground states. We apply a third pump laser, Pump 3, tuned to the two-photon resonance with Pump 2, as shown in Fig. 2c. A configuration for CPT is created in the **M**-system as recently studied in atomic systems[26] consisting of states 2, 6, 3, 8 and 4, such that a coherent state comprising all three triplet states is formed, with the probability amplitudes of individual states dictated by the relative intensities of the pumps and the relevant optical dipole moments. This is the first report of coherent control in a 5 level system in semiconductors and provides a novel platform for studies in electromagnetically-induced transparency.

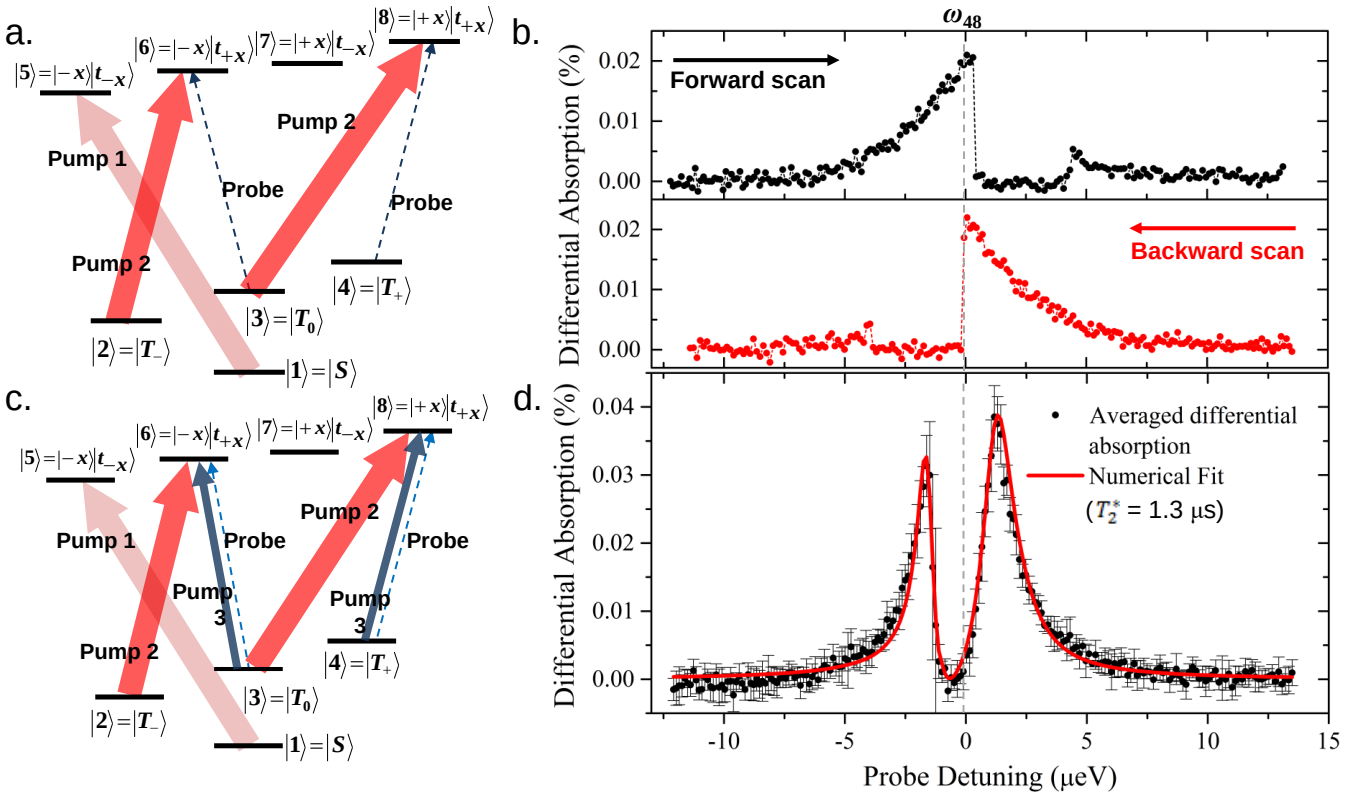

FIG. 2. Suppression of DNSP by optical nuclear spin locking. a. Pump configuration for T_+ state preparation. b. Probe absorption spectra following the pumping scheme in a. Upper(lower) panel: forward(backward) direction scan across $\omega_{48/36}$. c. Nuclear spin narrowing pump configuration d. Probe absorption spectrum showing the recovery of dark-state profile. Solid circles in the plot represent averaged data points obtained from 7 scans, error bars show standard deviations. Red solid line is the theoretical fit.

For the effective intensity ratio of Pump 2 to Pump 3 arbitrarily chosen to be 25 : 1, the system is coherently initialized to predominantly T_+ state. The Overhauser field is stabilized when the Rabi frequency of Pump 3 is adjusted to be sufficiently strong in order to overwhelm the dynamics induced by the scanning probe; the change in ground state population due to the probe is no longer significant enough to induce DNSP effects. As revealed in Fig. 2d, a prominent dark state dip is now observed and the distortion in the lineshape is suppressed. This allows us to simulate the behavior of the system without considering the effects of DNSP [22]. The full depth of the CPT dip indicates long ground state decoherence times, T_2^*, found to be at least 1.3 μs, corresponding to an extension by a factor of 500 compared to the estimated decoherence time due to thermally-distributed nuclear fluctuations[15], signifying a dramatic suppression of Overhauser field fluctuations in both QDs. *The nuclear spin quieting is nonlocal due to the fact that optical excitations occur only in the top QD.*

A unique feature of QDMs is that the spin-zero singlet state enables the experimental study of the roles of T_- and T_+ states in nuclear spin locking, as well as the direct observation of the associated quieting of Overhauser field distribution. In the pump configuration shown in Fig. 3a, the system is prepared in a coherent superposition of the singlet and T_+ state when Pump 2 and Pump 3 are in two-photon resonance. In the measured probe absorption spectrum (hollow circles in Fig. 3b), a dark-state dip is seen in each of the singlet transitions, as expected from the CPT. The lineshapes deviate from the ideal dark-state profile, while the depths of the dark-state dips in both transitions increase as the intensity of Pump 3 is raised. Without Pump 3, however, the system is prepared in the singlet state and the dark-state dips vanish (triangles in Fig. 3b) in the now broadened lineshapes, contrary to what is expected from CPT in a Λ-system, assuming an extended coherence time between the ground states [22]. This can be explained by considering a stochastic effective magnetic environment due to fluctuations in the nuclear spins of the underlying lattice. Although the singlet state is unaffected by the Overhauser field, the fluctuating Overhauser field affects both the spin-polarized top-QD trion, and the T_- and T_+ states, via the Zeeman shift, obscuring any dark state dip. To construct a theoretical fit, we assume a spectral diffusion model where the Overhauser field is assumed to

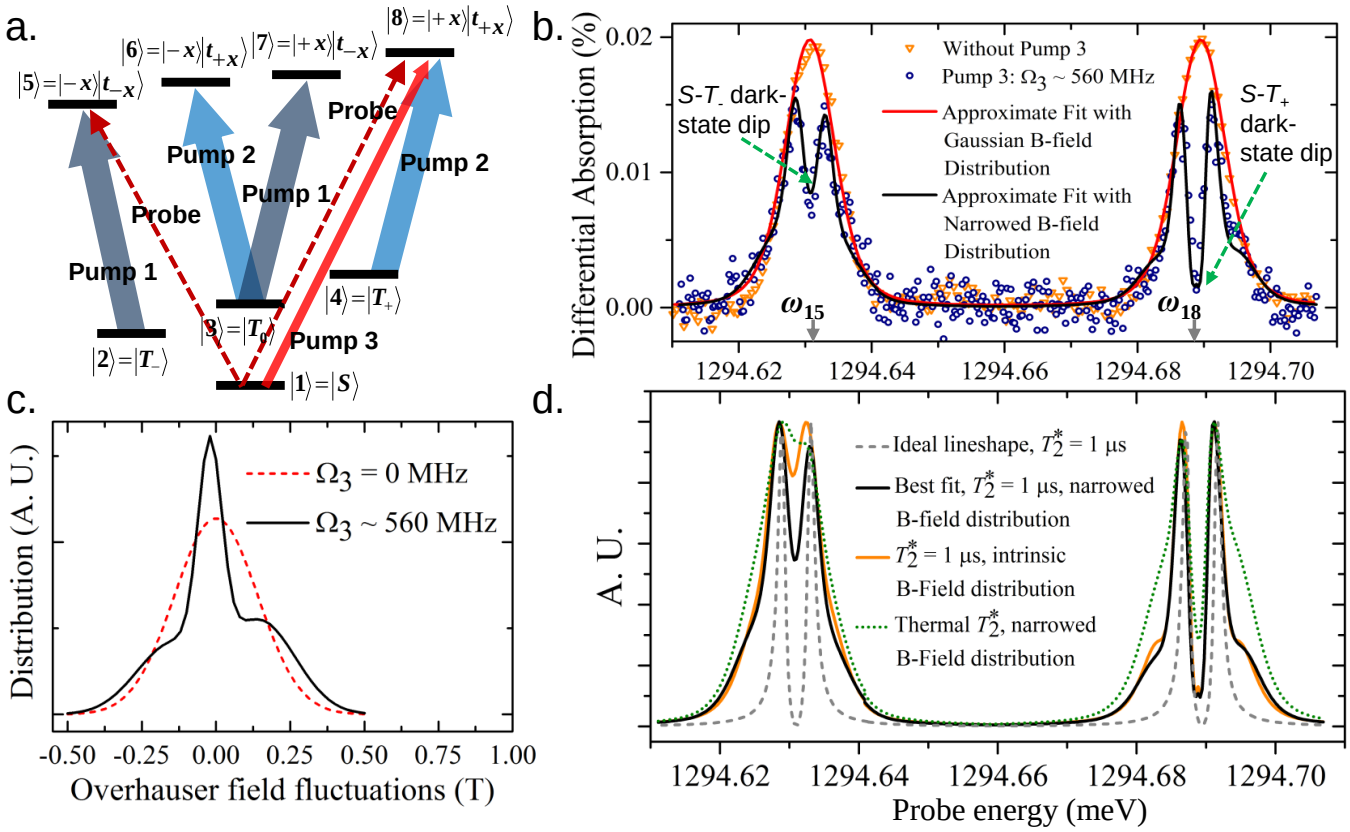

FIG. 3. Singlet-triplet coherence and nuclear field distribution quieting. a. Pump configuration for preparation of a coherent S-T_+ superposition. b. Absorption spectra showing the emergence of dark-state dips from S-T_- and S-T_+ coherence at transitions ω_{15} and ω_{18}, respectively with the application of Pump 3. c. Nuclear field distributions used in the numerical model for fitting the spectra in b. d. Comparison between spectra calculated from different combinations of decoherence times and Overhauser field distributions.

be slowly varying compared to optical processes[27]. The calculated absorption spectra corresponding to different individual Overhauser fields are then averaged according to the best-fitting Overhauser field distribution. Here the intrinsic Overhauser field (the case without Pump 3) follows a Gaussian distribution with an extracted standard deviation of 134 ± 50 mT (dashed line in Fig. 3c), in agreement with the theoretical order-of-magnitude estimate of 100 mT [22]. The resulting lineshape, shown as the red solid line in Fig. 3b, suggests that the averaging of different spectra is sufficient to obscure the dark-state dip as observed in both simulation and experiment, without invoking enhanced nuclear spin fluctuations.

Remarkably, when Pump 3 is applied, the same fitting procedure produces a narrowed distribution of the Overhauser field, as shown by the solid line in Fig. 3c, and reproduces the observed dark-state profiles of the two singlet transitions simultaneously. The appearance of both dark-state dips signifies a long spin decoherence time between the optical ground states, here estimated to be about 1 μs. This interpretation is corroborated by our simulations with different scenarios as described in Fig. 3d. In particular, for two limiting cases where in the first, an intrinsic Overhauser field distribution together with a long T_2^* of 1 μs is assumed, and in the second, a narrowed Overhauser field distribution with a thermal spin decoherence time of 2.5 ns[15], neither of the resulting lineshapes fits the data. Our model also accounts for the difference in the depths of the dips, where the dark-state dip at ω_{15} is shallower due to the finite width of the Overhauser field, while at ω_{18}, the dip is enhanced by Pump 3 which saturates the optical transition. We have no definitive explanation of the three-peak line shape of the Overhauser field distribution in the pumped case and relegate some possible interpretations in the Supplement[22]. In sum, the data presented in Fig. 3b along with lineshape analysis provides an experimental means to determine the Overhauser field quieting following optically-induced nuclear spin polarization via a nonzero T_+ population but we do not have the theory to support the field distribution.

The experimental results presented in this Letter indicate that the global nuclear spin ensemble composed of the two spatially separated nuclear spin ensembles in

different QDs can be stabilized via optical excitation in just one of the QDs mediated by the strong Coulomb exchange interaction. We envision a set of time-domain experiments in which a nuclear spin quieting stage precedes coherent spin manipulation and the coherence times of the two spins are measured independently. This experiment will allow us to determine the amount of time required to quiet the global nuclear spin ensemble, as well as the nuclear spin polarization decay rate in the presence of coherent control of the two electron spins. Previous work in single QD systems indicates that the electron spin coherence can be extended to at least a few hundred milliseconds [28] and that this coherence time extension persists in the absence of stabilizing lasers for at least 1.2 seconds [16].

In conclusion, we have demonstrated new degrees of freedom for coherently manipulating the electronic spin states and the underlying nuclear spin ensemble in a coupled-quantum dot system. The important new physics includes the observation that the nuclear spin quieting leads to ground state decoherence times in excess of 1.3 microseconds without recourse to dynamical decoupling and extends over both QDs, even though the driving of the hyperfine coupling via the optical excitation is localized to only one of the dots. The non-local nature of the DNSP effect over both dots stems from the strong exchange coupling, which could be reasonably attributed as the cause for electron-mediated nuclear spin flip-flop in two spatially separated QDs[13, 29–31]. Nuclear spin diffusion directly across the tunneling barrier between the QDs may need to overcome the strain-caused mismatch in nuclear Zeeman energy [13, 28, 32, 33]. Nevertheless, the underlying mechanisms of DNSP in QDMs are yet to be fully elucidated. Based on the nuclear spin quieting experiment presented here, the essential quantum information protocol separates the quieting period for stabilizing the nuclear destruction of the electron spin coherence from the subsequent quantum operations.

This work is supported by the following grants: NSF PHY 1104446, PHY 1413821, NSF PHY 1413956, AFOSR FA9550-09-1-0457, ARO W911NF-08-1-0487, DARPA FA8750-12-2-0333, ARO-MURI W911NF-09-1-0406.

[1] M. Atatüre, J. Dreiser, A. Badolato, A. Högele, K. Karrai, and A. Imamoglu, Science **312**, 551 (2006).
[2] X. Xu, Y. Wu, B. Sun, Q. Huang, J. Cheng, D. G. Steel, A. S. Bracker, D. Gammon, C. Emary, and L. J. Sham, Phys. Rev. Lett. **99**, 097401 (2007).
[3] A. J. Brash, L. M. P. P. Martins, F. Liu, J. H. Quilter, A. J. Ramsay, M. S. Skolnick, and A. M. Fox, Phys. Rev. Lett. **114**, 137401 (2015).
[4] D. Press, T. D. Ladd, B. Zhang, and Y. Yamamoto, Nat. Phys. **456**, 218 (2008).
[5] A. Greilich, S. E. Economou, S. Spatzek, D. R. Yakovlev, D. Reuter, A. D. Wieck, T. L. Reinecke, and M. Bayer, Nat. Phys. **5**, 262 (2009).
[6] E. D. Kim, K. Truex, X. Xu, B. Sun, D. G. Steel, A. S. Bracker, D. Gammon, and L. J. Sham, Phys. Rev. Lett. **104**, 167401 (2010).
[7] J. R. Schaibley, A. P. Burgers, G. A. McCracken, L. M. Duan, P. R. Berman, D. G. Steel, A. S. Bracker, D. Gammon, and L. J. Sham, Phys. Rev. Lett. **110**, 167401 (2013).
[8] K. De Greve, L. Yu, P. L. McMahon, J. S. Pelc, C. M. Natarajan, N. Y. Kim, E. Abe, S. Maier, C. Schneider, M. Kamp, S. Höfling, R. H. Hadfield, A. Forchel, M. M. Fejer, and Y. Yamamoto, Nature **491**, 421 (2012).
[9] W. B. Gao, P. Fallahi, E. Togan, J. Miguel-Sanchez, and A. Imamoglu, Nature **491**, 426 (2012).
[10] A. V. Kuhlmann, J. Houel, A. Ludwig, L. Greuter, D. Reuter, A. D. Wieck, M. Poggio, and R. J. Warburton, Nat. Phys. **9**, 570 (2013).
[11] M. J. Stanley, C. Matthiesen, J. Hansom, C. Le Gall, C. H. H. Schulte, E. Clarke, and M. Atatüre, Phys. Rev. B **90**, 195305 (2014).
[12] C. Matthiesen, M. J. Stanley, M. Hugues, E. Clarke, and M. Atatüre, Sci. Rep. **4**, 4911 (2014).
[13] B. Urbaszek, X. Marie, T. Amand, O. Krebs, P. Voisin, P. Maletinsky, A. Högele, and A. Imamoglu, Rev. Mod. Phys. **85**, 79 (2013).
[14] D. Press, K. De Greve, P. L. McMahon, T. D. Ladd, B. Friess, C. Schneider, M. Kamp, S. Höfling, A. Forchel, and Y. Yamamoto, Nat. Photonics **4**, 367 (2010).
[15] X. Xu, W. Yao, B. Sun, D. G. Steel, A. S. Bracker, D. Gammon, and L. J. Sham, Nature **459**, 1105 (2009).
[16] B. Sun, C. M. Chow, D. G. Steel, A. S. Bracker, D. Gammon, and L. J. Sham, Phys. Rev. Lett. **108**, 187401 (2012).
[17] E. A. Stinaff, M. Scheibner, A. S. Bracker, I. V. Ponomarev, V. L. Korenev, M. E. Ware, M. Doty, T. L. Reinecke, and D. Gammon, Science **311**, 636 (2006).
[18] M. F. Doty, M. Scheibner, A. S. Bracker, I. V. Ponomarev, T. L. Reinecke, and D. Gammon, Phys. Rev. B **78**, 115316 (2008).
[19] L. Robledo, J. M. Elzerman, G. Jundt, M. Atatüre, A. Högele, S. Fält, and A. Imamoglu, Science **320**, 772 (2008).
[20] D. Kim, S. G. Carter, A. Greilich, A. S. Bracker, and D. Gammon, Nat. Phys. **7**, 24 (2010).
[21] K. M. Weiss, J. M. Elzerman, Y. L. Delley, J. Miguel-Sanchez, and A. Imamoglu, Phys. Rev. Lett. **109**, 107401 (2012).
[22] See supplementary material at `http://google.com` including references [34–38]
[38] W. Liu, S. Sanwlani, R. Hazbun, J. Kolodzey, A. S. Bracker, D. Gammon, and M. F. Doty, Phys. Rev. B **84**, 121304(R) (2011).
[24] A. Greilich, S. C. Badescu, D. Kim, A. S. Bracker, and D. Gammon, Phys. Rev. Lett. **110**, 117402 (2013).
[25] X. Xu, B. Sun, P. R. Berman, D. G. Steel, A. S. Bracker, D. Gammon, and L. J. Sham, Nat. Phys. **4**, 692 (2008).
[26] Y. Gu, L. Wang, K. Wang, C. Yang, and Q. Gong, J. Phys. B **39**, 463 (2006).
[27] H. Wang and D. G. Steel, Phys. Rev. A **43**, 3823 (1991).
[28] E. A. Chekhovich, M. Hopkinson, M. S. Skolnick, and A. I. Tartakovskii, Nat. Commun. **6**, 6348 (2014).

[29] C. Deng and X. Hu, Phys. Rev. B **72**, 165333 (2005).
[30] C. W. Huang and X. Hu, Phys. Rev. B **81**, 205304 (2010).
[31] C. Latta, A. Srivastava, and A. Imamoglu, Phys. Rev. Lett. **107**, 167401 (2011).
[32] P. Maletinsky, M. Kroner, and A. Imamoglu, Nat. Phys. **5**, 407 (2009).
[33] E. A. Chekhovich, K. V. Kavokin, J. Puebla, A. B. Krysa, M. Hopkinson, A. D. Andreev, A. M. Sanchez, R. Beanland, M. S. Skolnick, and A. I. Tartakovskii, Nat. Nanotech. **7**, 646 (2012).
[34] P. R. Berman and V. S. Malinovsky, *Principles of laser spectroscopy and quantum optics* (Princeton University Press, 2011).
[35] C. Slichter, *Principles of Magnetic Resonance*, Springer Series in Solid-State Sciences (Springer Berlin Heidelberg, 1996).
[36] W. Yang and L. J. Sham, Phys. Rev. B **88**, 235304 (2013).
[37] M. Y. Petrov, I. V. Ignatiev, S. V. Poltavtsev, A. Greilich, A. Bauschulte, D. R. Yakovlev, and M. Bayer, Phys. Rev. B **78**, 045315 (2008).
[38] N. J. Stone, Atomic Data and Nuclear Data Tables **90**, 75 (2005).